Vahid Hassani, et. al. International Journal of Engineering Research and Applications
www.ijera.com
ISSN: 2248-9622, Vol. 11, Issue 2, (Series-VI) February 2021, pp. 37-58

RESEARCH ARTICLE OPEN ACCESS

A Comparison between Parametric Structural Optimization Methods and Software-Based Topology Optimization of A Rectangular Sample Under Tensile Load for Additive Manufacturing Processes

Vahid Hassani[1], Hamid Ahmad Mehrabi[2], Zunaidi Ibrahim[3], Iñigo Flores Ituarte[4]

[1]*Sustainable Advanced Manufacturing (SAM), University of Sunderland,vahid.hassani@sunderland.ac.uk*
[2]*Sustainable Advanced Manufacturing (SAM), University of Sunderland,hamid.mehrabi@sunderland.ac.uk*
[3]*Universiti Teknologi Brunei,zunaidi.ibrahim@utb.edu.bn*
[4]*Tampere University,inigofloresituarte@tuni.fi*
[1]*Vahid Hassani, https://orcid.org/0000-0001-6724-2520*
[2]*Hamid Ahmad Mehrabi, https://orcid.org/0000-0003-0510-4055*
[3]*Zunaidi Ibrahim, https://orcid.org/0000-0002-0246-1017*
[4]*Iñigo Flores Ituarte, https://orcid.org/0000-0002-1940-7527*

ABSTRACT
This article presents three methods of structural optimization for a rectangular sample under tensile load to minimize von Mises stress as an objective function. In the first method, namely the position-finding method, the initial volume is reduced by cut-extrusion of some circular holes with a uniform volume gradient along the length of the sample. In this method, the position of each hole is manipulated by using a genetic algorithm (GA) to achieve the minimum von Mises stress versus a specific tensile load. In the second method, namely geometry optimization method, several circular holes with different diameters are cut-extruded with monotonically decreasing volume gradient along the length of the sample to create a volume fraction at the beginning of optimization. As an alternative approach to the first method, an algorithm is seeded to alter the diameters of holes on the sample to minimize the same objective function i.e., von Mises stress. In the third method, namely integrated position and geometry optimization approach, severalsquare holes are cut-extruded along the length of the sample with a uniform volume gradient. Then, by using a GA, the position of each square along the width of the sample is manipulated together with their dimensions to minimize the same objective function of former methods versus the same applied load. Finally, the structural resultsof each sample in addition to the generated support structures, as one of the basic elements of some additive manufacturing (AM) processes,are compared with the software-based topologically-optimized sample with equivalent volume fraction.

Keywords: Structural Optimization; Topology Optimization; Additive Manufacturing (AM); Support Structures;

Date of Submission: 16-02-2021 Date of Acceptance: 02-03-2021

I. INTRODUCTION

In the last decades, several methods have been presented for solving the structural optimization problem of structures and mechanical systems [1-4]. These approaches have specifically used different optimization algorithms, either heuristic or metaheuristic, to generally find the optimum configuration, shape, and size of the structures and components. In this field of research, some examples such as a node-shifting method for improvement of the stiffness of spatial structures [5], multi-objective metaheuristic optimization for design improvement of a twist drill [6], two-phase GA and evolutionary computing for geometry optimization of a roof structure [7] can be enumerated.

Among the different methods of structural optimization, topology optimization has recently attracted much interest across research teams and industry sectors thank the emergence of additive manufacturing (AM) technologies [8]. Currently, AM excels for the creation of several products, which cannot be easily built by conventional manufacturing methods [9, 10]. Knowing the unique

capability of AM i.e., building the parts with complex geometry inspires engineers from different fields to use topology optimization technique, which is one of the main sources of complexities in the design of components [11]. In the literature, a wide range of applications of topology optimization are observed such as fiber orientation of composites by using topology optimization [12, 13], multi-material [14] and multi-scale topology optimization [15], topology optimization for heat transfer enhancement [16-19], topology optimization for sound absorbing application [20] and topology optimization of piezoelectric-based energy harvester [21].

However, the applications of topology optimization are not necessarily confined to those mentioned above and the wider applications can be found in the field of AM technologies. Basically, topology optimization is often used to reduce material usage; and therefore, manufacturing time and cost in AM [22]. Alternatively, in different framework, topology optimization was used to design support structure for laser powder bed fusion as one of the processes of metal AM to prevent residual stress-induced build failure during the process [23]. Some AM processes like fusion deposition modeling (FDM) induce anisotropic behavior in the printed objects, meanwhile along different build orientations, the printed part will exhibit different mechanical properties that have sometimes negative effects on the functionality of the part. To mitigate the effect of anisotropicity, strength-based topology optimization was presented [24] as a new methodology. By using topology optimization, a multifunctional part was designed and optimized such that both structural and system requirements were considered [25]. In this line of research, a design process was presented for compliance-based minimization of topologically-optimized lattice structure [26]. Also, topology optimization was used as a method of generating a self-supporting structure of AM processes to reduce the post-processing cost and time to remove the excessive generated support structure [27]. The enclosed voids in the design of the printed parts in metal AM were avoided by using topology optimization in the powder bed fusion process to remove and reuse unmelted metal powder [28]. In this context, the concept of multi-component topology optimization for powder bed AM was proposed mainly to eliminate enclosed voids during the process [29]. For the first time, topology optimization of steel 3d printed structure was proposed for connecting nodesin space frames by Ren and Galjaard [30]. In thermofluid applications, the thermo-fluid topology optimization in the design of conformal cooling channels and injection molding was considered [31]. In another research, the topology optimization approach was used as an algorithm for finding the distribution of hard and soft polymers in a rectangular sample under different tensile load scenarios for printing in a multi-material voxel 3d printer [32].

Despitewide applications of topology optimization mentioned above, there are still some manufacturing limitations that restrict the use of this technique by engineers and researchers. As discussed earlier, a topologically-optimized part can mostly be built by using AM processes, which are neither yet accessible anywhere nor economical.Furthermore, in some cases, a topologically-optimized part needs to be rationalized [11, 33] to be easily printable by 3d printers and also consumes less time and cost for post-processing subtractive operation, particularly in the metal printing process. Understanding these issues, this paper aims to propose quasi-topology optimization methods by which an optimization algorithm is seeded on a simple configuration i.e., a rectangular sample that has an identical volume fraction of the equivalent topologically-optimized sample. These methodsenable engineers and researchers to implement and generalize it on the parts and components that have simple or moderately simple configurations, regardless of inaccessibility to AM processes, meanwhile, it can be even realized by conventional manufacturing methods [22].The authors will also show that the proposed optimization methods in this study will offer betterperformance over the topology optimization method in terms of the generated support structures as one of the basic elements of some AM processes.

This paper is organized into four sections. In Section 2, the initial configuration of three samples, respectively for three optimization methods, are sketched and a finite element analysis (FEA) will be performed on them as pre-optimization analysis. In Section 3, the three optimization methods will be discussed and compared with equivalent software-based topology optimization in detail. Finally, the conclusion of the paper will be discussed in Section 4.

II. INITIAL SKETCHING AND PRE-OPTIMIZATION ANALYSIS OF RECTANGULAR SAMPLES

This section describes the sketching procedure of the three samples which will be used for three methods of structural optimization, namely position-finding method, Geometry Optimization method, and integrated position and geometry optimization approach. These methods will be discussed in Section 3.

2.1. Sample Sketching for Position-Finding Method

For this purpose, we use the SolidWorks environment to sketch simply a rectangular sample. Firstly, a rectangle witha 110mm overall length and 25mm width is sketched and extruded to create 4mm thickness. This sample is partitioned into three subsections in which the first 25mm of the sample's length is chosen as grip section or boundary condition of the fixed support, the middle part with 60mm length is chosen as a target area in which the 18 circular holes with equal diameters are cut-extruded and the last 25mm of sample's length is chosen as load section to apply the external tensile load on it. The middle section or target area is the main part of the sample in which the structural optimization is performed. This section, which in turn, is divided into six equal subsections (columns) with 10mm length. Inside each subsection, three circles are cut-extruded with diameters of 5mm along the sample's width, which formsa totallyof 18 circular holes. This number is purposefully pre-determined to create the desired volume fraction i.e., 24% in the target area. Figure 1 shows the different partitions of the rectangular sample with their dimensions. In this sketch, the volume gradient along the length of the sample will remain constant, as the diameters of all circular holes are identical and structural optimization algorithm will not make any change on the diameters of the holes, but only change their initial positions.

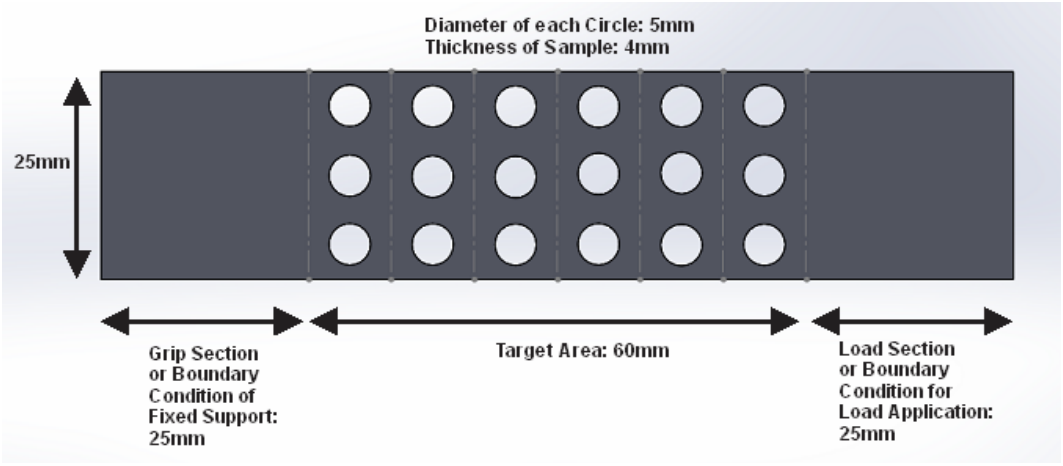

Figure 1. Rectangular Sample for the Position-Finding Method

To perform the pre-optimization FE analysisof the sample, HP 3D High Reusability PA 12 material was assigned to the sample, which is used in the form of powder in HP 3d printers. The main properties of the material areshown in Table 1.

Table 1. Mechanical Properties of HP 3D High Reusability PA 12

Mechanical Properties	Quantity
Young's Modulus	**1700 MPa**
Yield Strength	**48 MPa**
Tensile Strength	**48 MPa**
Poisson's Ratio	**0.35**
Density	**1010 kg/m^3**

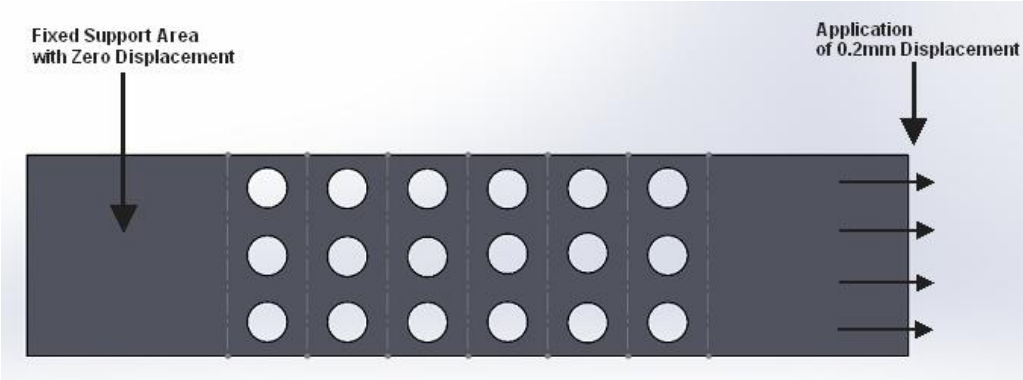

Figure 2. Boundary Condition and Applied Displacement

After material selection, the first 25mm of the sample's length (grip section) is chosen as fixed boundary condition with zero displacements and rotation and the last 25mm of the sample's length (load section) is chosen as an area for applying the displacement input of 0.2mm along the length of the sample as tensile load, which is shown in Figure 2. Figures 3a and 3b show the results of static analysis of the sample before optimization at COMSOL software asan FEA tool. The maximum von Mises stress and the maximum total displacement are 15.5 MPa and 0.2 mm, respectively.

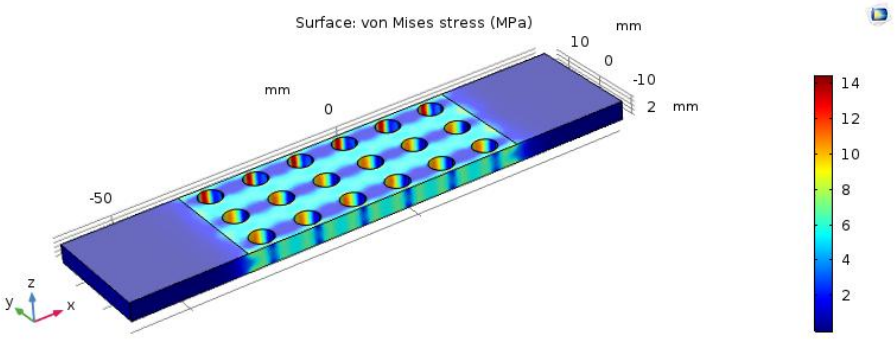

a)

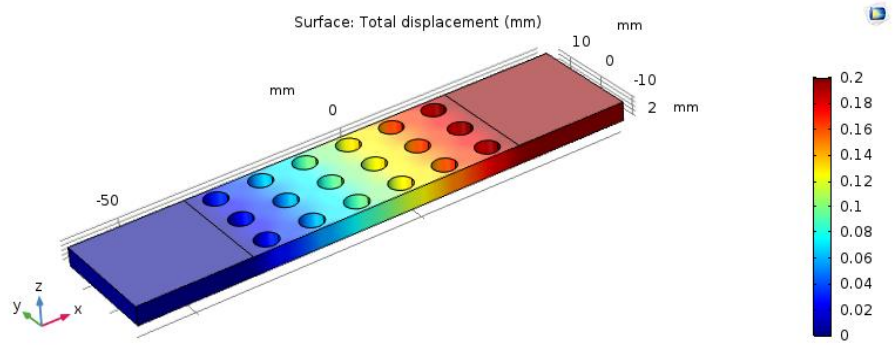

b)

Figure 3. Results of Static Analysis, a) von Mises Stress: 15.5 MPa, b) Displacement: 0.2mm

2.2. Sample Sketching for Geometry Optimization Method

In this section, we use the SolidWorks environment to sketch simply a rectangular sample similar to the former method. Repeatedly, at first, a rectangle with 110mm overall length and 25mm width is sketched and extruded to create 4mm thickness. This sample is partitioned into three subsections in which the first 25mm of the sample's length is chosen as grip section or boundary condition of the fixed support, the middle part with 60mm length is chosen as a target area in which the

18 circular holes with different diameters are cut-extruded and the last 25mm of sample's length is chosen as load section to apply the external tensile load on it. The middle section or target area is the main part of the sample in which the structural optimization is performed. This section, which in turn, is divided into six equal subsections (columns) with 10mm length. Inside each subsection, three circles are cut-extruded with diameters of 5mm, 4mm, 3mm, 2mm, 1mm, and 0.8mm along the sample's width, subsequently. Figure 4 shows the different partitions of the rectangular sample with their dimensions. In this sketch, the volume gradient along the length of the sample will decrease uniformly, as the diameters of all circular holes are varying along the length ofthe target area. In this method, the structural optimization algorithm will make a change on the initial volume fraction of target area, since the diameters of holes vary during the optimization process. The final obtained volume fraction after the optimization process will be considered to compare with the equivalent topologically-optimized sample.

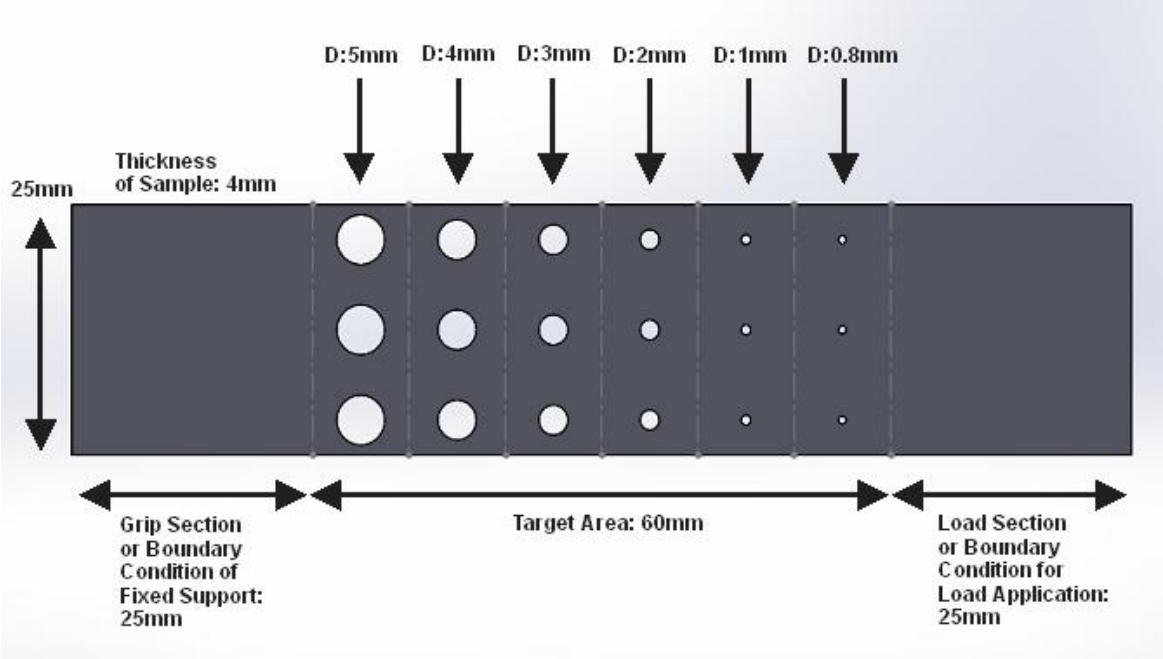

Figure 4. Rectangular Sample for the Geometry Optimization Method

Similarly, to perform the pre-optimization FE analysis of the sample, HP 3D High Reusability PA 12 material was assigned to the sample, which is used in the form of powder in HP 3d printers. The main properties of the material are shown in Table 1.

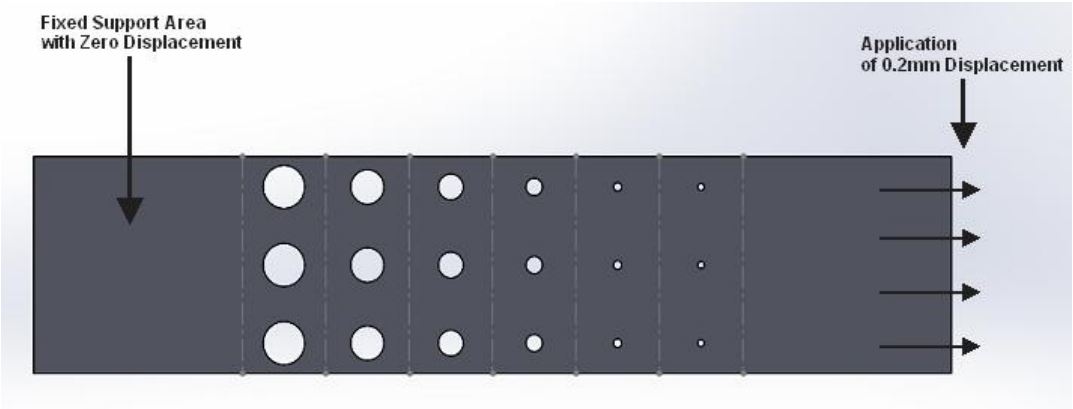

Figure 5. Boundary Condition and Applied Displacement

After material selection, the first 25mm of the sample's length (grip section) is chosen as fixed boundary condition with zero displacements and rotation and the last 25mm of the sample's length (load section) is chosen as an area for applying the displacement input of 0.2mm along the length of the sample as tensile load, which is shown in Figure 5. Figures 6a and 6b show the results of static analysis of the sample before optimization at COMSOL software as an FEA tool. The maximum von Mises stress and the maximum total displacement are 22.8 MPa and 0.2 mm, respectively.

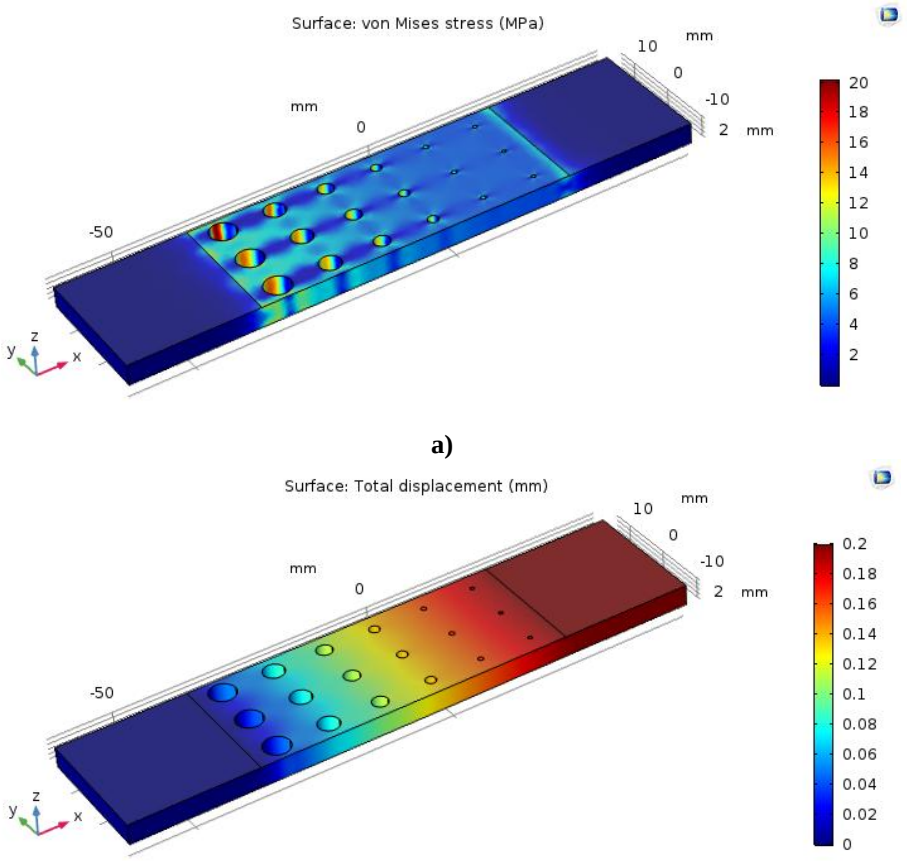

a)

b)

Figure 6. Results of Static Analysis, a) von Mises Stress: 22.8 MPa, b) Displacement: 0.2mm

2.3. Sample Sketching for Integrated Position and Geometry Optimization Approach

In this section, we use the SolidWorks environment to sketch simply a rectangular sample similar to former methods. Similarly, at first, a rectangle witha 110mm overall length and 25mm width is sketched and extruded to create 4mm thickness. This sample is partitioned into three subsections in which the first 25mm of the sample's length is chosen as grip section or boundary condition of the fixed support, the middle part with 60mm length is chosen as a target area in which the 6squareslots with equal dimensions are cut-extruded and the last 25mm of sample's length is chosen as load section to apply the external tensile load on it. The middle section or target area is the main part of the sample in which the structural optimization is performed. This section, which in turn, is divided into six equal subsections (columns) with 10mm length. Inside each subsection, one squareis cut-extruded with dimensions of 5mm*5mm. Figure 7 shows the different partitions of the rectangular sample with their dimensions. In this sketch, the volume gradient along the length of the sample will be constant at the beginning of the optimization process, but as the dimensions of all square slots are varying during the optimization process, the volume fraction will change, respectively. The final obtained volume fraction after the optimization process will be considered to compare with the equivalent topologically-optimized sample.

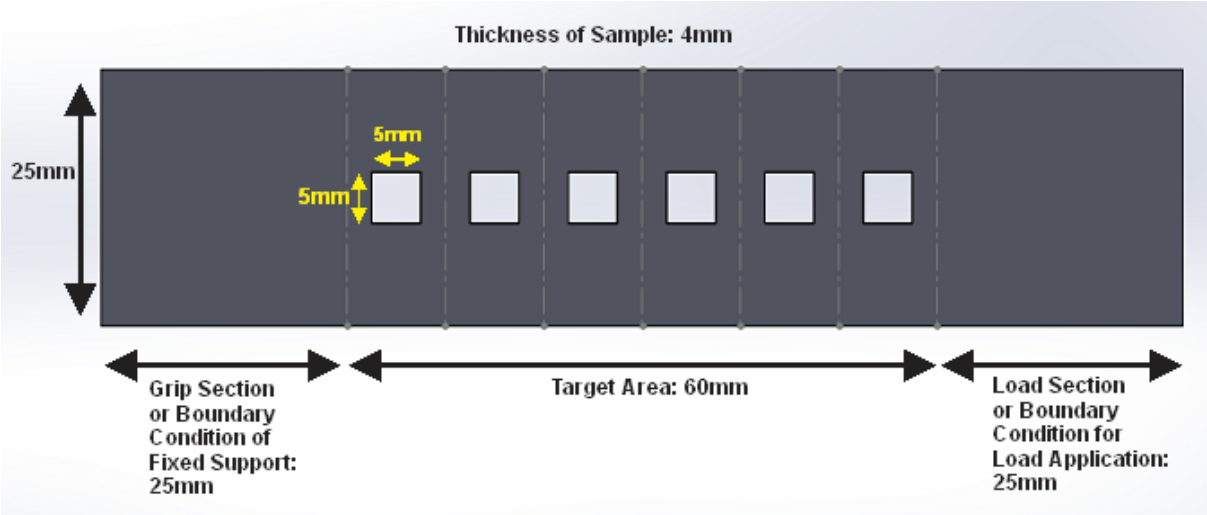

Figure 7. Rectangular Sample for Integrated Position and Geometry Optimization Approach

To perform the pre-optimization FE analysis of the sample, HP 3D High Reusability PA 12 material was assigned to the sample, which is used in the form of powder in HP 3d printers. The main properties of the material are shown in Table 1.

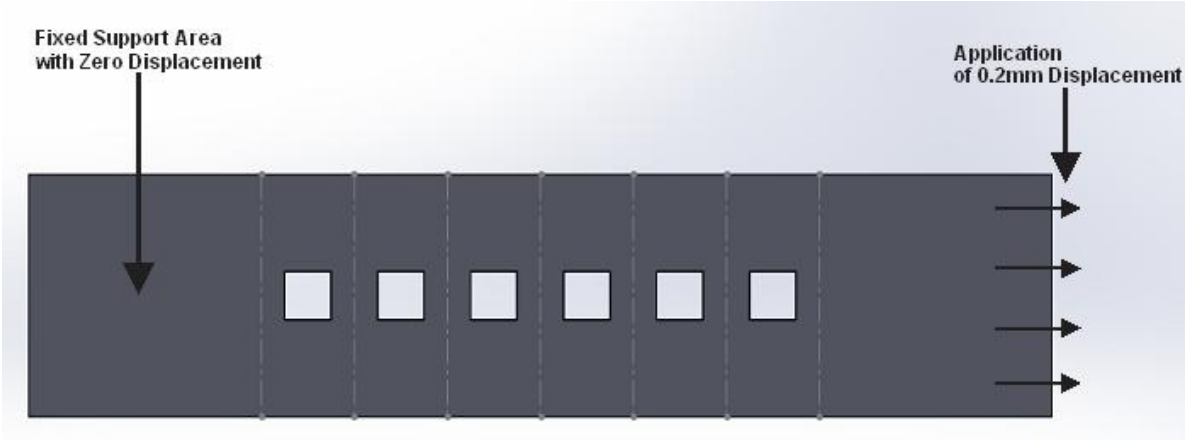

Figure 8. Boundary Condition and Applied Displacement

After material selection, the first 25mm of the sample's length (grip section) is chosen as fixed boundary condition with zero displacements and rotation and the last 25mm of the sample's length (load section) is chosen as an area for applying the displacement input of 0.2mm along the length of a sample as tensile load, which is shown in Figure 8. Figures 9a and 9b show the results of static analysis of the sample before optimization at COMSOL software as an FEA tool. The maximum von Mises stress and the maximum total displacement are 12 MPa and 0.2 mm, respectively.

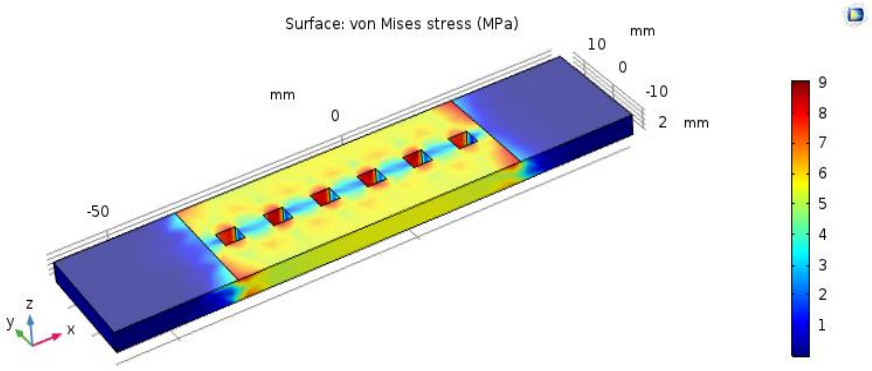

a)

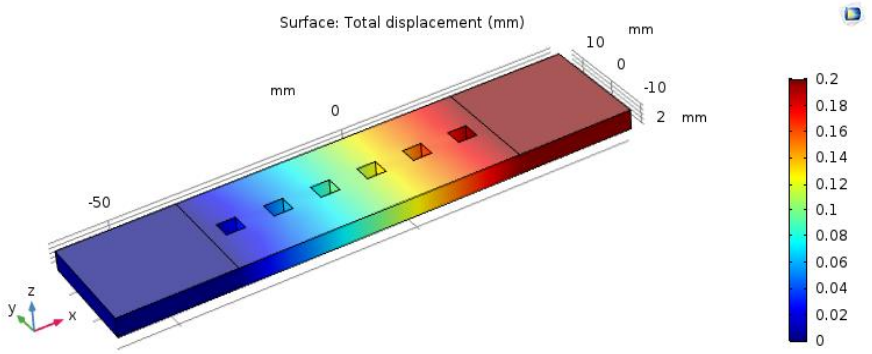

b)

Figure 9. Results of Static Analysis, a) von Mises Stress: 12 MPa, b) Displacement: 0.2mm

III. STRUCTURAL OPTIMIZATION METHODS AND COMPARISON WITH TOPOLOGY OPTIMIZATION

This section is devoted to describing the three optimization methods, namely the position-finding method, geometry optimization method, and integrated position and geometry optimization approach. The design method is implemented through interlink among three software: SolidWorks, MATLAB, and COMSOL. As workflow shows in Figure 10, initial sketching is performed in SolidWorks that was discussed comprehensively in Section 2, then transitions to COMSOL for FEAand MATLAB for optimization as shown in Figure 10.

3.1. Structural Optimization using Position-Finding Method

In this method, first of all, the parameters of optimization have to be determined. As the name of the method suggests, the longitudinal position of each circular hole is chosen as the parameters for the optimization process. The initial position of each hole is set to be in the middle of each subsection of the target area i.e., 5mm from datum lines as shown in Figure 11.

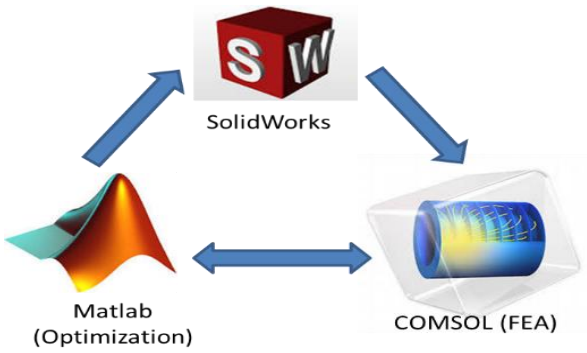

Figure 10. Interlink Triangle between Three Software [34]

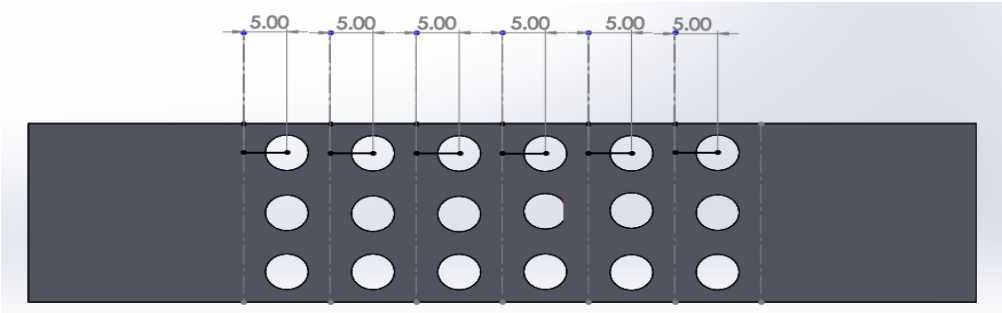

Figure 11. Initial Position of each Circular Hole from Datum line

These holes are allowed to travel 3mm to right and left sides of hole centers, meanwhile, the lower bound of parameters are chosen 2mm and the upper bounds are chosen 8mm concerning datum lines. Arrows in Figure 12 show the longitudinal travel in the desired range from left to right and vice versa.

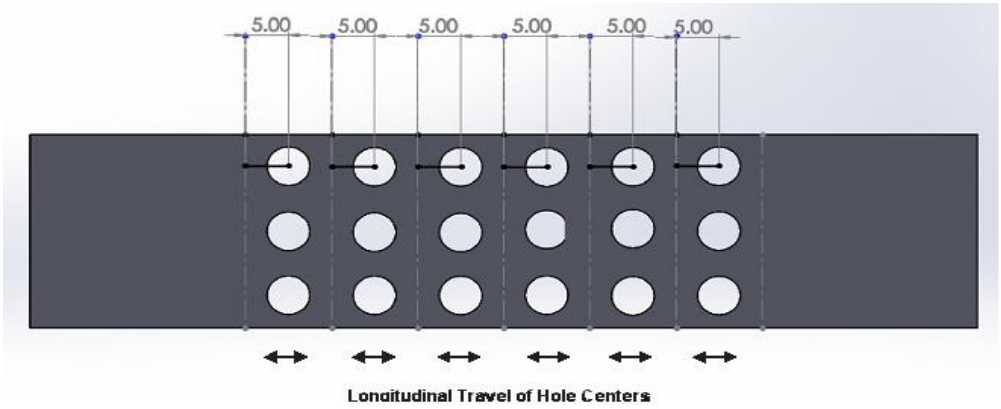

Figure 12. Longitudinal Travel of each Hole Centre between Lower and Upper Bounds

After the determination of the design parameters, the structural optimization problem can be defined as the optimization of a real objective function *f*, which depends on the hole parameters and is subjected to some constraints. After the above discussion, the minimization problem is defined as:

Min $f(x)$

Subject to $g_j(x) \le 0, j=1,m$ (1)

$$h_k(x) = 0, k = 1, l$$

$$x_i^l \le x_i \le x_i^u, i = 1, n$$

where $x = [x_1, ..., x_n]$ is the vector of design parameters, $f(x)$ is the objective function, $g_j(x)$ are the inequality constraint, $h_k(x)$ are the equality constraints and x_i^l and x_i^u are lower and upper bounds of the i^{th} design variable respectively.

In this research, we select the maximum von Mises stress as the objective function. To specialize equation (1) to the current structural optimization problem, the general form of the equation is rewritten by the following functions shown in Table 2.

Table 2. Formulation of Optimization Problem for Position-Finding Method

Given	Material,Boundary Conditions (B.C), Loads
Find	X_i: The i^{th} distance betweendatum linesand i^{th}hole center point.
Satisfy	$X_i^l \le X_i \le X_i^u$: Lower and upper bounds of parameters.
Minimize	Max σ_{von_Mises} : Maximum von Mises Stress

Given the boundary conditions, B.C, loads shown in Figure 2 and Material information given in Table 1, the distances between datum lines and hole center points, X_i, will be optimized within the structural optimization process. The static characteristics of the sample such as maximum von Mises stress, maximum total displacement, etc. are measured using a finite element analysis (FEA). The initial values, X_i's are set midst of each subsection at the target area, an analysis is performed using the COMSOL software as an FEA tool. The same displacement input is applied to the sample as shown in Figure 2. In this analysis, a mesh is built for the sample at each iteration using the "fine" setting. Linear tetrahedral elements were used uniformly with an average element quality of 0.8 and minimum element quality of 0.1 for the sample at the beginning of the optimization process. The sample under analysis is a single solid part that is simulated in the elastic range, meanwhile, there is no large deformation occurring through the analysis. Asa result, the optimization module in COMSOL software will adaptively update the coordinates and orientation of meshes during the optimization process depending on the new configuration of the holes at every iteration.

From the results of the pre-optimization analysis and static characteristics of the sample shown in Figure 3, the optimization process was pursued until the smaller von Mises was obtained compared to the initial configuration of the sample. The final optimized structure is illustrated in Figure 13 and the results of the optimization process are shown in figures 14a and 14b. The updated values are compared in Table 3 for the positions of hole centers before and after the optimization process.The maximum von Mises stress and the maximum total displacement are 14.5 MPa and 0.2 mm, respectively.

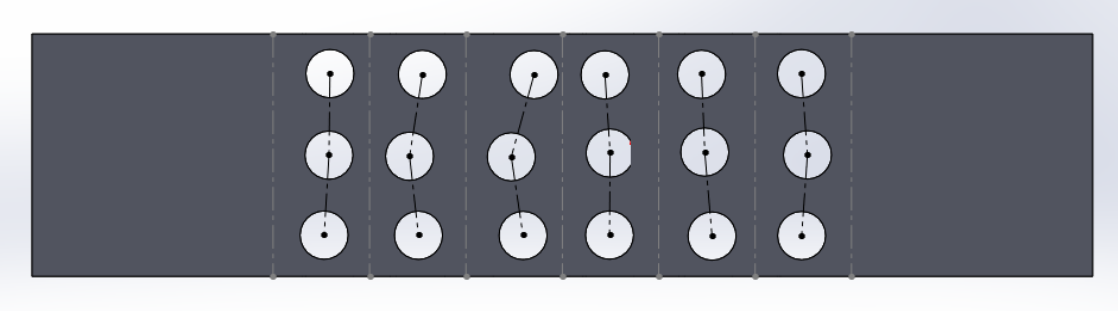

Figure 13. New Positions of Hole Centers after Optimization Process

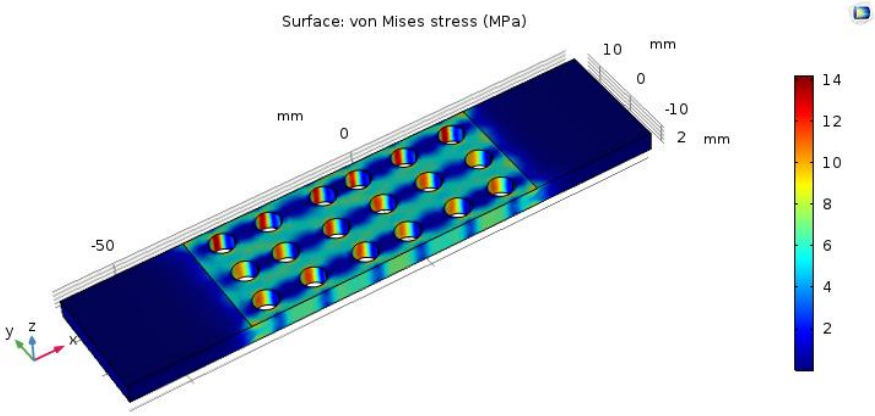

a)

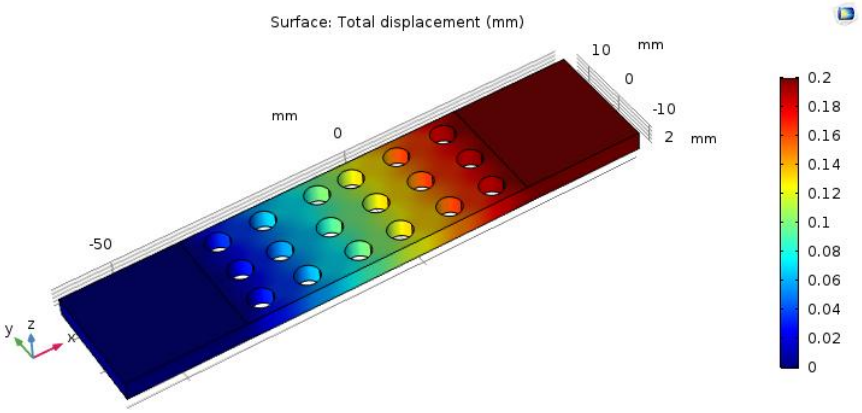

b)

Figure 14. Results of Static Analysis after Optimization Process, a) von Mises Stress: 14.5 MPa, b) Displacement: 0.2mm

The optimization process was performed using a genetic algorithm in MATLAB optimization toolbox with the settings as, the population size of 200, Tournament selection method, single-point crossover with a rate of 0.8, adaptive feasible mutation with a rate of 0.01 and 500 iterations.

Table 3. Comparison between Positions of Hole Centers before and after Optimization Process

Column Numbers from Left to Right of Target Area	**Column 1**	**Column 2**	**Column 3**	**Column 4**	**Column 5**	**Column 6**
Before Optimization	5mm 5mm 5mm	5mm 5mm 5mm	5mm 5mm 5mm	5mm 5mm 5mm	5mm 5mm 5mm	5mm 5mm 5mm
After Optimization	5.9mm 5.8mm 5.3mm	5.5mm 4.2mm 5.1mm	7.1mm 4.7mm 5.9mm	4.4mm 5.0mm 4.9mm	4.5mm 4.8mm 5.5mm	4.8mm 5.7mm 4.8mm

It appears the improvement of the structural characteristics of the sample after the optimization process. The maximum von Mises stress has a decrease of almost 7% and the safety factor has an increase of 7% that ensures the higher safety margin for the sample.

To compare the different optimization methods, one software-based topology optimization was performed under the same boundary condition and displacement input shown in Figure 2. The volume fraction of 24% was chosen as a constraint of the problem, which is equal to the volume fraction of the position-finding method. As illustrated in Figure 15, the maximum value obtained for the maximum von Mises stress is 15.3 MPa that is slightly higher than the value obtained after optimization by the position-finding method.

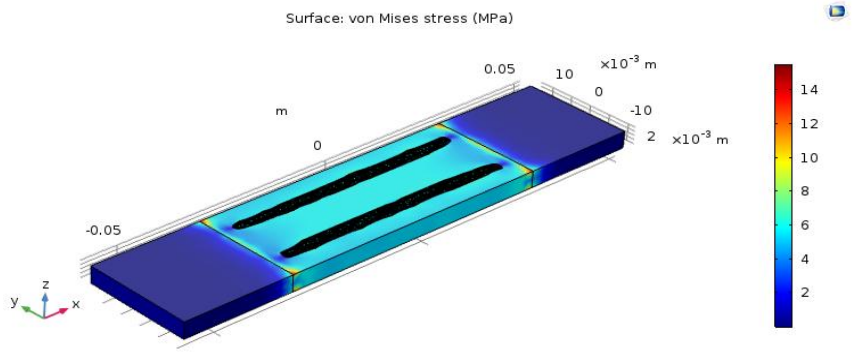

Figure 15. Result of Topology Optimization, von Mises Stress: 15.3 MPa

The final configuration of the sample after topology optimization is also shown in Figure 16.

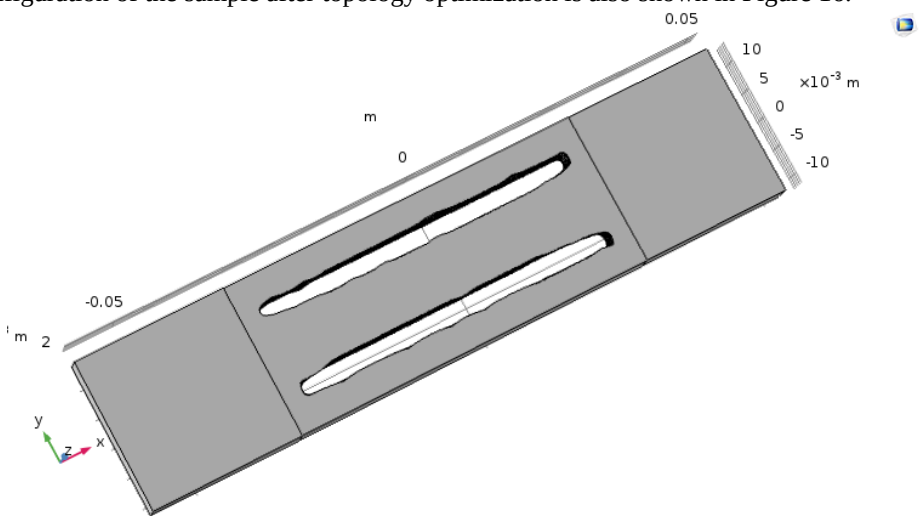

Figure 16. Final Configuration of the Sample after Topology Optimization with 24% Volume Fraction as Constraint

3.2. Structural Optimization using Geometry Optimization Method

In this method, the diameters of the circular holes are chosen as the parameters of structural optimization. The diameters of the circular holes are allowed to vary between 1mm and 7mm, meanwhile, the lower bound of parameters are chosen 1mm and the upper bounds are chosen 7mm. Similarly, the maximum von Mises stress of the sample is selected as the objective function. To specialize equation (1) to the current structural optimization problem, the general form of the equation is rewritten by the following functions shown in Table 4.

Table 4. Formulation of Optimization Problem for Geometry Optimization Method

Given	Material, Boundary Conditions (B.C), Loads
Find	X_i: The i^{th}diameter of the circular holes
Satisfy	$X_i^l \leq X_i \leq X_i^u$: Lower and upper bounds of parameters.
Minimize	Max σ_{von_Mises} : Maximum von Mises Stress

Given the boundary conditions, B.C, loads shown in Figure 5 and Material information given in Table 1, the diameters of the circular holes, X_i, will be optimized within the structural optimization process. The static characteristics of the sample such as maximum von Mises stress, maximum total displacement, etc. are measured using a finite element analysis (FEA). The initial values, X_i's are set, as shown in Figure 4, an analysis is performed using the COMSOL software as an FEA tool. The same displacement input is applied to the sample as shown in Figure 5. In this analysis, a mesh is built for the sample at each iteration using the "fine" setting. Linear tetrahedral elements were used uniformly with an average element quality of 0.9 and minimum element quality of 0.06 for the sample at the beginning of the optimization process. The sample under analysis is a single solid part that is simulated in the elastic range, meanwhile, there is no large deformation occurring through the analysis. Asa result, the optimization module in COMSOL software will adaptively update the coordinates and orientation of meshes during the optimization process depending on the new configuration of the holes at every iteration.

From the results of the pre-optimization analysis and static characteristics of the sample shown in Figure 6, the optimization process was pursued until the smaller von Mises was obtained compared to the initial configuration of the sample. The final optimized structure is illustrated in Figure 17 and the results of the optimization process are

shown in figures 18a and 18b. The updated values are compared in Table 5 for the diameters of holes before and after the optimization process. The maximum von Mises stress and the maximum total displacement are 20 MPa and 0.2 mm, respectively.

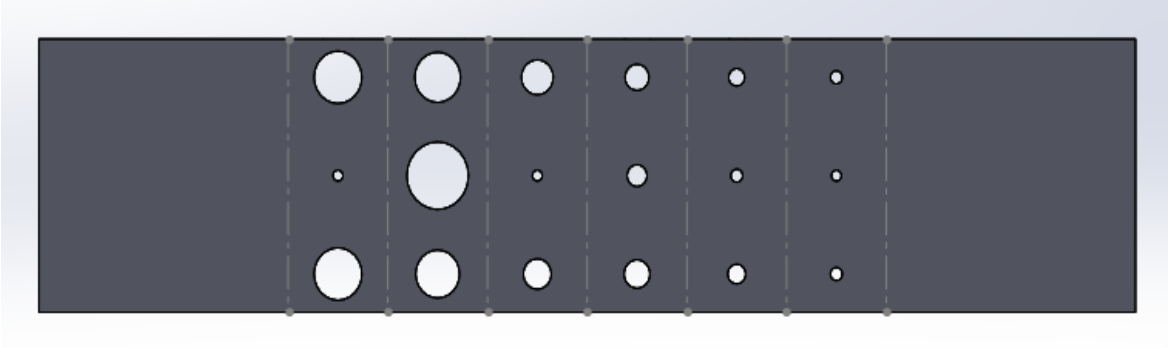

Figure 17. New Diameters of the Circular Holes after Optimization Process

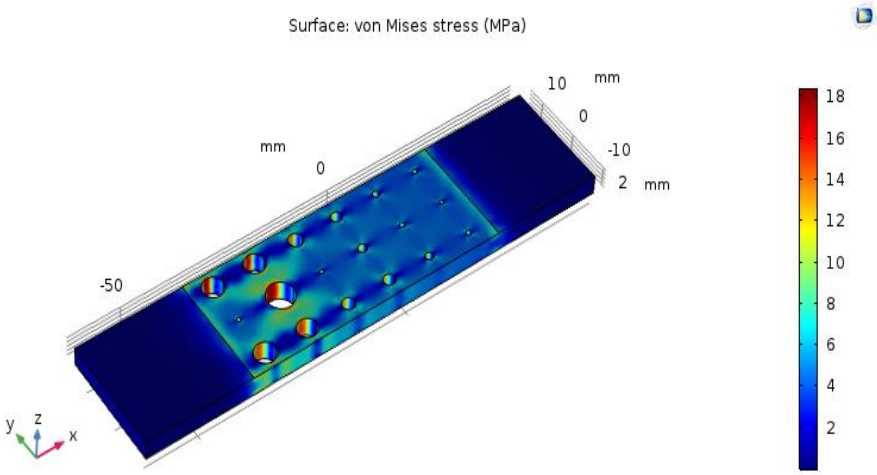

a)

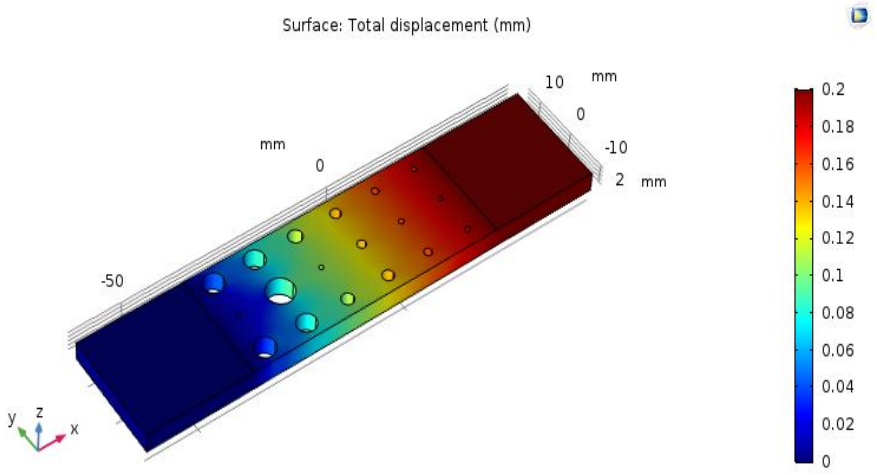

b)

Figure 18. Results of Static Analysis after Optimization Process, a) von Mises Stress: 20 MPa, b) Displacement: 0.2mm

With the same settings of optimization toolbox in MATLAB, discussed in Section 3.1, the optimization process was performed.

Table 5. Comparison between Diameters of Circular Holes before and after Optimization Process

Column Numbers from Left to Right of Target Area	Column 1	Column 2	Column 3	Column 4	Column 5	Column 6
Before Optimization	5mm 5mm 5mm	4mm 4mm 4mm	3mm 3mm 3mm	2mm 2mm 2mm	1mm 1mm 1mm	0.8mm 0.8mm 0.8mm
After Optimization	4.8mm 1.0mm 4.8mm	4.6mm 6.2mm 4.4mm	3.2mm 1.0mm 2.8mm	2.4mm 2.0mm 2.6mm	1.6mm 1.2mm 1.8mm	1.2mm 1.0mm 1.2mm

It appears the improvement of the structural characteristics of the sample after the optimization process.The maximum von Mises stress has a decrease of almost 12.3% and the safety factor has an increase of 14.2% that ensures the higher safety margin for the sample.

To compare the different optimization methods, one software-based topology optimization was performed under the same boundary condition and displacement input shown in Figure 5. The volume fraction of 10% was chosen as a constraint of the problem, which is equal to the volume fraction of the sample after the geometry optimization method. As illustrated in Figure 19, the maximum value obtained for the maximum von Mises stress is 16.6 MPa that is lower than the value obtained after optimization by geometry optimization method.

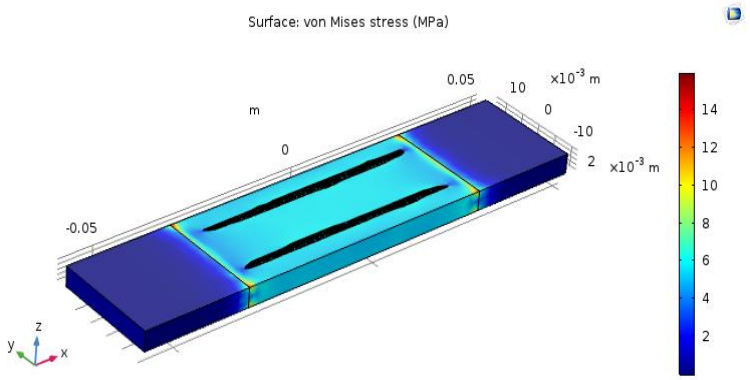

Figure 19. Result of Topology Optimization, von Mises Stress: 16.6 MPa

The final configuration of the sample after topology optimization is also shown in Figure 20.

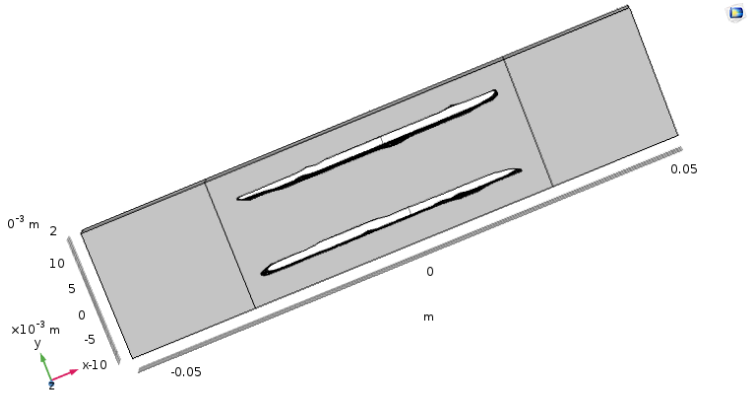

Figure 20. Final Configuration of the Sample after Topology Optimization with 10% Volume Fraction as Constraint

3.3. Structural Optimization by Integrated Position and Geometry Optimization Approach

In this method, two sets of parameters were determined for the structural optimization process. One set includes the distance from the lower edge of the sample to the lower edges of squares as shown in Figure 21 and the other set includes the dimensions of the six squares, length, and width as shown in Figure 7.

Figure 21. The Distance from the Lower Edges of the Sample and the Lower Edges of Squares

The initial values of parameters for the first set are chosen 10mm, which locates the center of each square in the centerline of the sample, and for the second set are chosen 5mm*5mm to form six squares with identical dimensions. The lower and upper bounds of the first set are chosen between 2mm from the lower edge of the sample and 16mm from the same edge. For the second set of parameters, the lower bound is chosen 3mm and the upper bound is chosen 7mm, respectively.

Given the boundary conditions, B.C, loads shown in Figure 8, and Material information given in Table 1, the distances from the lower edge of the sample to the lower edges of the squares and the dimensions of the square, X_i, will be optimized within the structural optimization process. The static characteristics of the sample such as maximum von Mises stress, maximum total displacement, etc. are measured using a finite element analysis (FEA). The initial values, X_i's are setmidst ofthetarget area, an analysis is performed using the COMSOL software as an FEA tool. The same displacement input is applied to the sample as shown in Figure 8. In this analysis, a mesh is built for the sample at each iteration using the "fine" setting. Linear tetrahedral elements were used uniformly with an average element quality of 0.85 and minimum element quality of 0.08 for the sample at the beginning of the optimization process. The sample under analysis is a single solid part that is simulated in the elastic range, meanwhile, there is no large deformation occurring through the analysis. Asa result, the optimization module in COMSOL software will adaptively update the coordinates and orientation of meshes during the optimization process depending on the new configuration of square slots at every iteration.

From the results of the pre-optimization analysis and static characteristics of the sample shown in Figure 9, the optimization process was pursued until the smaller von Mises was obtained compared to the initial configuration of the sample. The final optimized structure is illustrated in figures22a, 22b, and 22c, and the results of the optimization process are shown in figures 23a and 23b. The updated values are compared in Table 6 for the positions and dimensions of square slots, before and after the optimization process. The maximum von Mises stress and the maximum total displacement are 8.5 MPa and 0.2 mm, respectively.

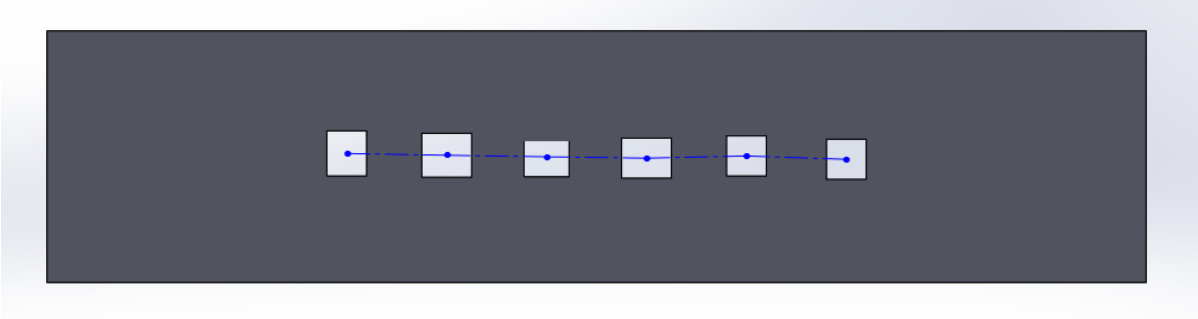

a)

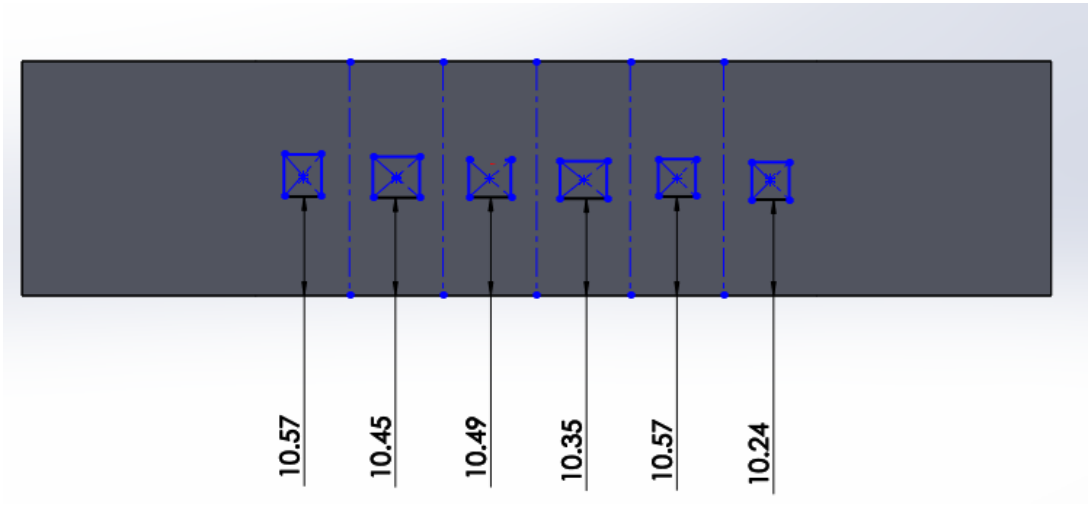

b)

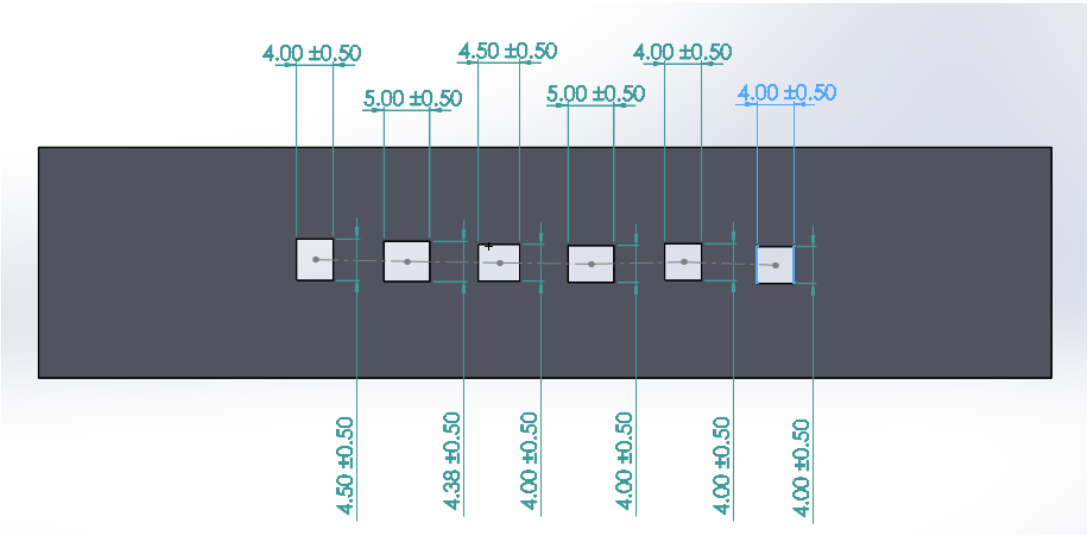

c)

Figure 22. The Resulting Optimized Structure, a) New Positions of Rectangles Relative to the Centerline of the Sample, b) New Positions from the Lower Edge of the Sample, c) New Dimensions of Rectangles

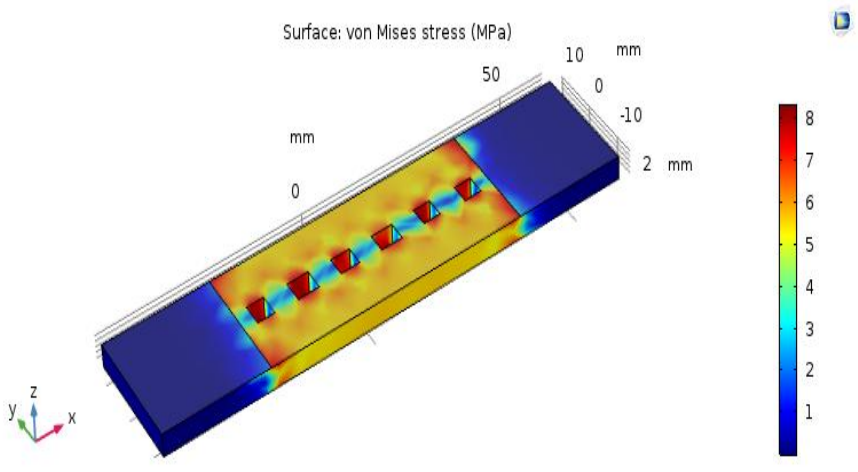

a)

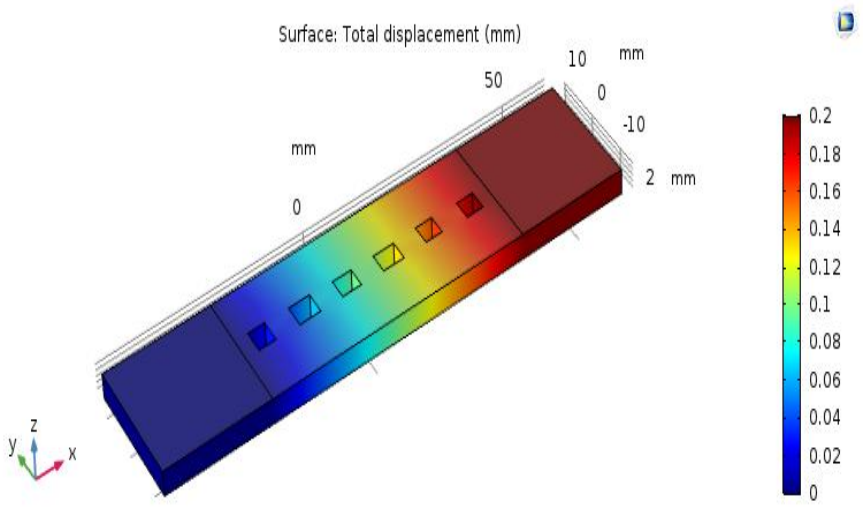

b)

Figure 23. Results of Static Analysis after Optimization Process, a) von Mises Stress: 8.5 MPa, b) Displacement: 0.2mm

With the same settings of optimization toolbox in MATLAB, discussed in Section 3.1, the optimization process was performed.

Table 6. Comparison between Parameters before and after Optimization Process

Column Numbers from Left to Right of Target Area	Column 1 Distance Length Width	Column 2 Distance Length Width	Column 3 Distance Length Width	Column 4 Distance Length Width	Column 5 Distance Length Width	Column 6 Distance Length Width
Before Optimization	10.0mm 5mm 5mm	10.0mm 5mm 5mm	10.0mm 5mm 5mm	10.0mm 5mm 5mm	10.0mm 5mm 5mm	10.0mm 5mm 5mm
After Optimization	10.57mm 4.5mm 5.0mm	10.45mm 5.5mm 4.88mm	10.49mm 5mm 4.5mm	10.35mm 5.5mm 4.5mm	10.57mm 4.5mm 4.5mm	10.24mm 4.5mm 4.5mm

It appears the improvement of the structural characteristics of the sample after the optimization process. The maximum Von-Mises stress has a decrease of almost 30% and the safety factor has an increase of 41% that ensures the higher safety margin for the sample.

To compare the different optimization methods, one software-based topology optimization was performed under the same boundary condition and displacement input shown in Figure 8. The volume fraction of 10% was chosen as a constraint of the problem, which is equal to the volume fraction of the sample after the integrated position and form-finding approach. As illustrated in Figure 19, the maximum value obtained for the maximum von Mises stress is 16.6 MPa that is quite higher than the value obtained after optimization by integrated position and form-finding approach.

3.4. Method Investigation

Overall comparison between the two methods of optimization, one parametric design, and another software-based topology optimization, will show that the flexibility in the design process for the former method is higher than the latter one i.e., software-based topology optimization. As appears,

two different methods discussed in sections 3.2 and 3.3 have given two different values for the objective function, one is higher than the topologically-optimized sample and another is much lower than the topologically-optimized sample with equivalent volume fraction of 10%. It means that shifting the design from circular hole feature to square slot has improved the results, however different geometric features may give better results after the optimization process, whereas the software-based topology optimization will not have that flexibility based on the load, boundary condition, and constraints defined for the optimization problem.In order to compare the compliance created in each method, one functional test was performed to measure the strain energy per unit volume. The lower value of strain energy will create more stiffness and less compliance. Among the different methods, it is obviously obsereved in Figure 24 that the integrated position and geometry optimization approach has created the highest stiffness with the least strain energy per unit volume and the geometry optimization method has created the maximum energy with the lowest stiffness, meanwhile it will be dofrmed more than other samples versus the identical tensile force applied to it. Both topologically-optimized samples are located in the middle part of plot with at least better stiffness characteristics compared to the sample that has been structurally optimized by geometry optimization method. But apart from the comparisons made above, for the design improvement of the parts and components with complex geometry, topology optimization, as a well-knownmethod for generative design, has already proved its unique capability for increasing the stiffness to weight ratio.

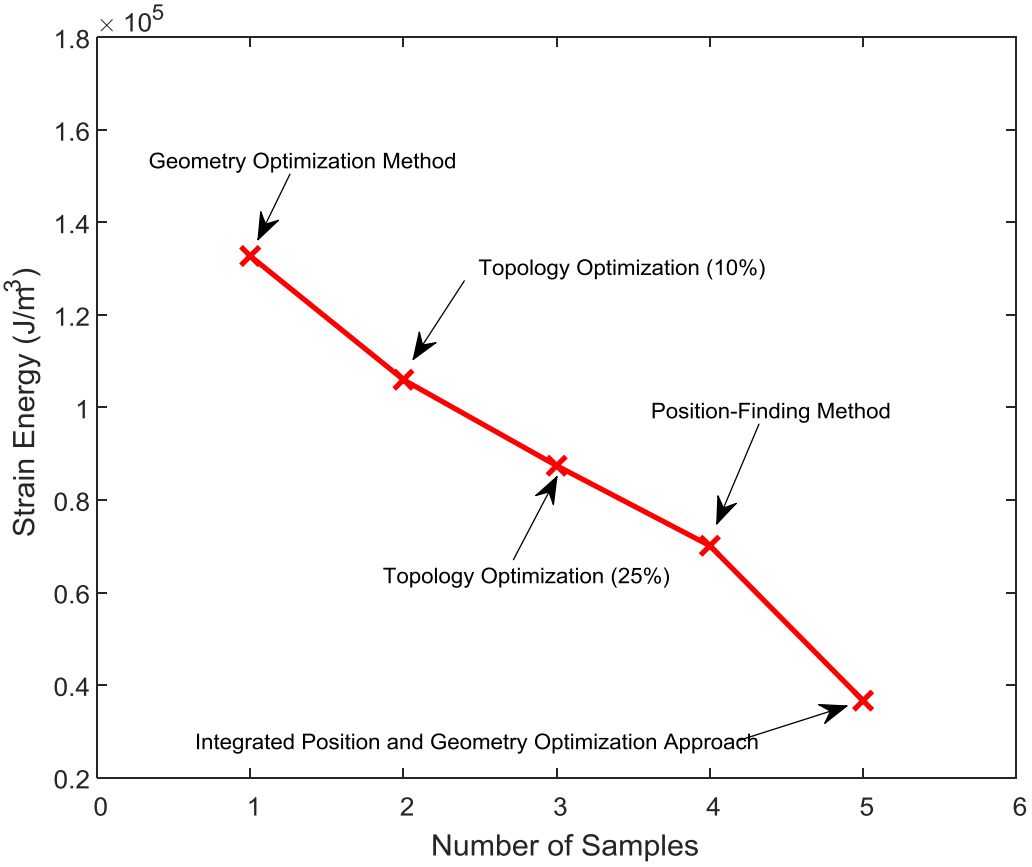

Figure 24. Comparison between Stiffness for each Sample in terms of Strain Energy per Unit Volume (J/m^3)

In another point of view, although conventional manufacturing methods mostly fail to build topologically-optimized parts, they can easily build the simple features like circular holes, square slots that have been shown in section 3.1, 3.2, 3.3. However, due to the unique capabilities of AM technologies, designers tend to build topologically-optimized parts with an increasing rate. Despite high demands for the design of topologically-optimized parts among the researchers and industries, AM

methods are yet under development and they also have some issues that need to be identified. Concerns such as support structure will create some difficulties mainly in the post-processing operations in terms of cost and time. As is well known, some AM processes require the use of support structures, specifically the metal AM, FDM (fusion deposition modeling), and Polyjet processes. Support structures are used to support bottom surfaces, overhangs, and internal cavities and channels (pipes, pipelines). The designer must consider supports during part design [35]. The role of support generation and support removal has equal importance during the additive and subtractive processes. The support has to be generated to ensure that the part is properly printed without any deformation, but the generated support must be removed in the subtractive process either using liquid solvents, manually, or by special machining tools. As shown in Figure 25, a topologically-optimized part, the support structure is hard to remove when it is generated in an irregular feature than a regular one such as circle, rectangle, or square. The sharp edges and dents can also be seen in figures 16 and 20 for the topologically-optimized sample under study in this research. If these samples have some orientations in the build platform at which the support structure is generated, the removal of the support structure will be cumbersome. To prove this issue evidently, one simulation was performed in Autodesk Netfabb software to evaluate the type of support structure generated in each sample when it is orientated in the build platform vertically in the XZ plane. As shown in figures 26 a-d, different types of support structures are created depending on the different features such as circular holes, square slots, and topologically-optimized one. In Figure 26a, since the diameter of the circular holes are equal, the support structure have the same configuration almost in all holes. In contrast, in the sample with different circular holes shown in Figure 26b, small circular holes have not been supported and it results in less time for post-processing operation and material used. In different features like square, the type of support structure is denser due to sharp corners of the square and consequently, the removal of support structure needs more accuracy to maintain the original feature safely. And finally, Figure 26d shows the topologically-optimized sample with the same orientation in the build platform that has a very dense support structure due to irregular and rough surface generated after performing the topology optimization. Obviously, this configuration claims more material as a support structure and its removal needs more accuracy and time.To have an accurate removal of such support structures, more precise and advanced machining devices are needed that claim more costs, time, and skilled operators.

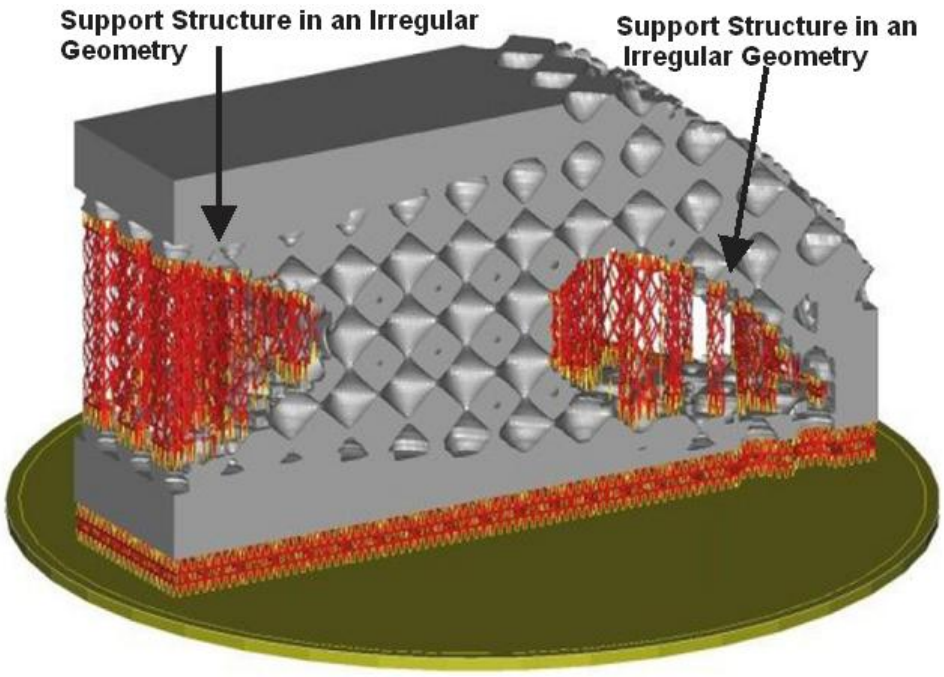

Figure 25. Support Structure in A Topologically-Optimized Part [36]

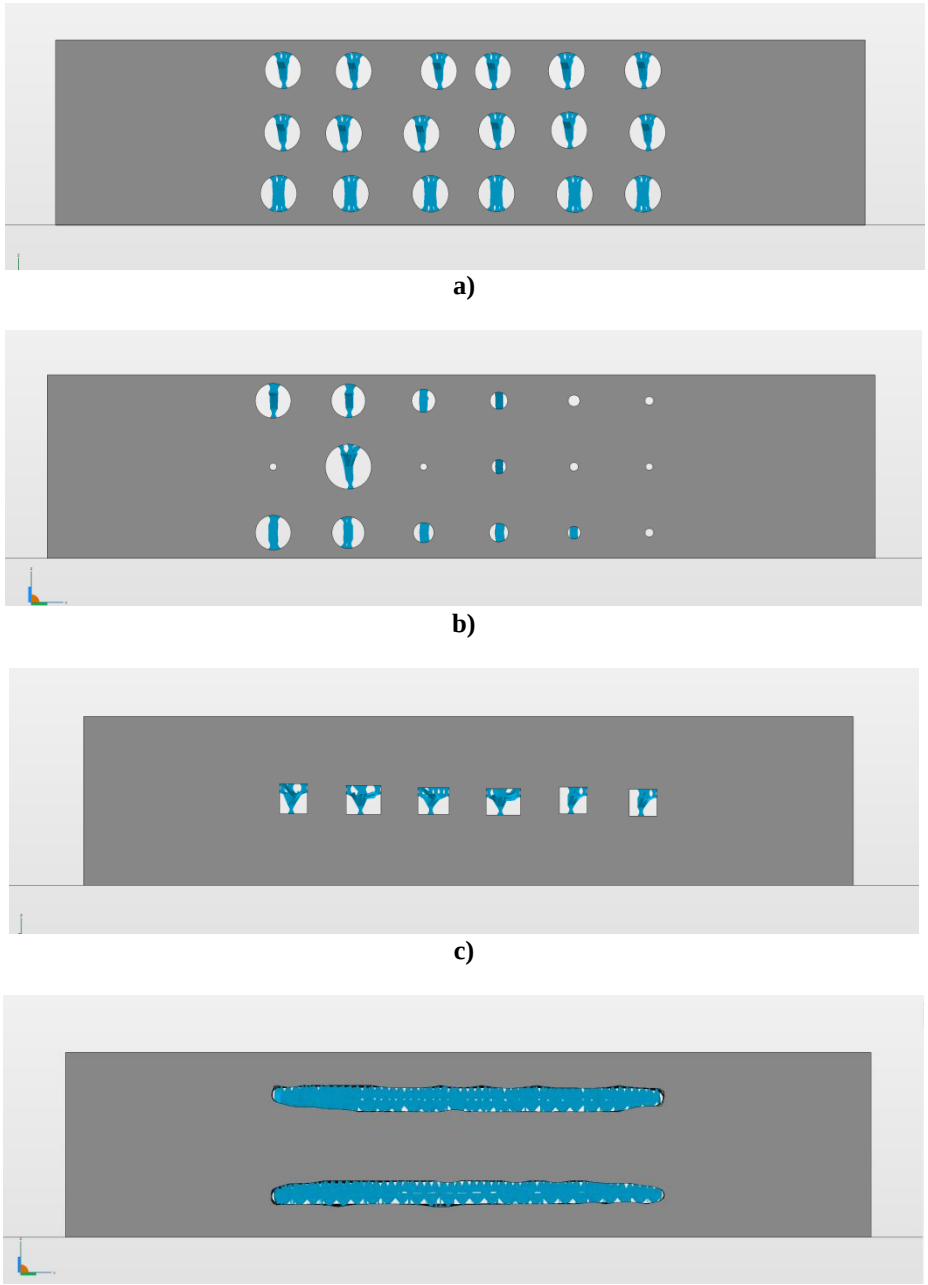

a)

b)

c)

d)

Figure 26. Support Structures (shown with blue color) at Different Samples, a) Position-Finding Method, b) Geometry Optimization Method, c) Integrated Position and Geometry Optimization Approach, d) Software-Based Topologically-Optimized Sample

IV. CONCLUSIONS

In this study, a simple rectangular sample was chosen as a working platform to demonstrate the three parametric methods of structural optimization and topology optimization. The parametric optimization process was initiated by sketching some particular features to create specific volume fractions in the rectangular samples. In the first method, the optimization process was pursued by optimizing the position of those features i.e., circular holes, while in the second method, the geometry of circular holes was manipulated to solve the structural optimization problem. Alternatively, an integrated approach of position and geometry optimization for different features compared to the first and second methods was proposed to increase the design freedom during the optimization process. Finally, some advantages of the proposed methods over the topology optimization were considered in terms of structural performance, design

flexibilityand the generated support structure from the viewpoint of post-processing operation of AM processes.

REFERENCES

[1]. V. Hassani, Z. Khabazi, F. Raspall, C. Banon, D. W. Rosen, Form-Finding and Structural Shape Optimization of the Metal 3D-Printed Multi-Branch Node with Complex Geometry, Journal of Computer-Aided Design and Applications (CADA), 17 (2019) 205-225.

[2]. L. -D. Thang, H. -H. Vinh, N. -T. Trung, N. -Q. Hung , A New Design Approach Based on Differential Evolution Algorithm for Geometric Optimization of Magnetorheological Brakes, Journal of Smart Materials and Structures, 25 (2008).

[3]. L. Zhichun, Z. Shiping, G. Ya, S. Feng, Z. Lingping, L. Wei, Geometric Optimization of Two-Stage Thermoelectric Generators using Simplified Conjugate-Gradient Method, Journal of Applied Energy, 190 (2017) 540-552.

[4]. Z. L. Guo, J. T. Tat, H. Y. Song, Y. Guilin, M. Sitti, Structural Optimization of Flexure-Based Parallel Mechanisms towards Achieving Optimal Dynamic and Stiffness Properties, Journal of Precision Engineering, 42 (2015) 195-207.

[5]. C. Ding, H. Seifi, S. Dong, Y. M. Xie,A New Node-Shifting Method for Shape Optimization of Reticulated Spatial Structures, Journal of Engineering Structures, 152 (2017) 727-735.

[6]. E. Abele, M. Fujara, Simulation-Based Twist Drill Design and Geometry Optimization, CIRP Annals-Manufacturing Technologies, 59 (2010) 145-150.

[7]. M. Kociecki, H. Adeli, Shape Optimization of Free-Form Space-Frame Roof Structures with Complex Geometries using Evolutionary Computing, Journal of Engineering Applications of Artificial Intelligence, 38 (2015) 168-182.

[8]. I. Gibson, D. W. Rosen, B. Stucker, Additive Manufacturing Technologies: Rapid Prototyping to Direct Digital Manufacturing, Second Edition, Springer, (2010).

[9]. V. Hassani, D. W. Rosen, E. Goh, S. Sarwan, F. Doetzer, A Design Method to Exploit Synergies between Fiber-Reinforce Composites and Additive Manufactured Processes, Solid Freeform Fabrication 2019: Proceedings of the 30th Annual International, (2019) 2015-2027.

[10]. V. Hassani, An Investigation of Additive Manufacturing Technologies for Development of End-Use Components: A Case Study, International Journal of Pressure Vessels and Piping, 187 (2020).

[11]. V. Hassani, Z. Khabazi, H. A. Mehrabi, C. Gregg, R. W. O'Brien, Rationalization Algorithm for A Topologically-Optimized Multi-Branch Node for Manufacturing by Metal Printing,Journal of Building Engineering,29 (2019).

[12]. T. Nomura, A. Kawamoto, T. Kondoh, E. M. Dede, J. Lee, Y. Song, N. Kikuchi, Inverse Design of Structure and Fiber Orientation by means of Topology Optimization with Tensor Field Variables, Journal of Composites: Part B, 176 (2019).

[13]. J. Lee, D. Kim, T. Nomura, E. M. Dede, J. Yoo, Topology Optimization for Continuous and Discrete Orientation Design of Functionally Graded Fiber-Reinforced Composite Structures, Journal of Composite Structures, 201(2018).

[14]. P. Liu, L. Shi, Z. Kang, Multi-Material Structural Topology Optimization Considering Material Interfacial Stress Constraints, Journal of Computer Methods in Applied Mechanics and Engineering, Singapore, 363 (2020).

[15]. J. C. Steuben, A. P. Iliopoulos, J. P. Michopoulos, Multiscale Topology Optimization for Additively Manufactured Objects, Journal of Computing and Information Science in Engineering, 18 (2018).

[16]. A. Pizzolato, A. Sharma, K. Maute, A. Sciacovelli, V. Verda, Topology Optimization for Heat Transfer Enhancement in Latent Heat Thermal Energy Storage, International Journal of Heat and Mass Transfer, 113 (2017).

[17]. C. Lundgaard, O. Sigmund, A Density-Based Topology Optimization Methodology for Thermoelectric Energy Conversion Problems, Journal of Structural and Multidisciplinary Optimization, 57 (2018) 1427-1442.

[18]. M. Zhou, J. Alexandersen, O. Sigmund, C. B. W. Pedersen, Industrial Application of Topology Optimization for Combined Conductive and Convective Heat Transfer Problems, Journal of Structural and Multidisciplinary Optimization, 54(2016) 1045-1060.

[19]. Z. Liu, W. -D. Lee, Y. -B. Wang, G. -Q. Su, G. -J. Zhang, Y. Cao, D. -C. Li, Topology Optimization and 3D-printing Fabrication Feasibility of High Voltage FGM Insulator, 2016 IEEE International Conference on High Voltage Engineering and Application

(ICHVE), September 19-22, 2016, Chengdu, China, (2016).

[20]. A. Takezawa, T. Yamamoto, X. Zhang, K. Yamakawa, S. Nakano, M. Kitamura, An Objective Function for the Topology Optimization of Sound-Absorbing Materials, Journal of Sound and Vibration, 443 (2019) 804-819.

[21]. A. H. Amlashi, A. M. Ousaid, M. Rakotondrabe, Topology Optimization of 2DOF Piezoelectric Plate Energy Harvester under External In-Plane Force, Journal of Micro-Bio Robotics, 47 (2020).

[22]. I. Flores, N. Kretzschmar, A. H. Azman, S. Chekurov, D. B. Pedersen, A. Chaudhuri, Implications of Lattice Structures on Economics and Productivity of Metal Powder Bed Fusion, Journal of Additive Manufacturing, 31 (2020) 100947.

[23]. L. Cheng, X. Liang, J. Bai, Q. Chen, J. Lemon, A. To, On Utilizing Topology Optimization to Design Support Structure to Prevent Residual Stress Induced Build Failure in Laser Powder Bed Metal Additive Manufacturing, Journal of Additive Manufacturing, 27 (2019) 290-304.

[24]. A. M. Mirzendehdel, B. Rankouhi, K. Suresh, Strength-Based Topology Optimization for Anisotropic Parts, Journal of Additive Manufacturing, 19 (2018) 104-113.

[25]. A. Panesar, I. Ashcroft, D. Brackett, R. Wildman, R. Hague,Design Framework for Multifunctional Additive Manufacturing: Coupled Optimization Strategy for Structures with Embedded Functional Systems, Journal of Additive Manufacturing, 16 (2017) 98-106.

[26]. J. Robbins, S. J. Owen, B. W. Clark, T. E. Voth, An Efficient and Scalable Approach for Generating Topologically Optimized Cellular Structures for Additive Manufacturing, Journal of Additive Manufacturing, 12 (2016) 296-304.

[27]. M. Langelaar, Topology Optimization of 3D Self-Supporting Structures for Additive Manufacturing, Journal of Additive Manufacturing, 12 (2016) 60-70.

[28]. Y. Xiong, S. Yao, Z. -L. Zhao, Y. M. Xie, A New Approach to Eliminating Enclosed Voids in Topology Optimization for Additive Manufacturing,Journal of Additive Manufacturing, 32 (2020).

[29]. Y. Zhou, T. Nomura, K. Saitou, Multi-Component Topology Optimization for Powder Bed Additive Manufacturing (MTO-A), Proceedings of the ASME 2018 International Design Engineering, Technical Conferences and Computers and Information in Engineering Conference, IDETC/CIE 2018, August 26-29, 2018, Quebec City, Quebec, Canada, (2018).

[30]. S. Ren, S. Galjaard, Topology Optimization for Steel Structural Design with Additive Manufacturing, Journal of Modeling Behavior, (2015) 35-44

[31]. T. Wu, A. Tovar, Design for Additive Manufacturing of Conformal Cooling Channels using Thermal-Fluid Topology Optimization and Application in Injection Molds, Proceedings of the ASME 2018 International Design Engineering, Technical Conferences and Computers and Information in Engineering Conference, IDETC/CIE 2018, August 26-29, 2018, Quebec City, Quebec, Canada, (2018).

[32]. I. F. Ituarte, N. Boddeti, V. Hassani, M. L. Dunn, D. W. Rosen, Design and Additive Manufacture of Functionally Graded Structures Based on Digital Materials, Journal of Additive Manufacturing, 30 (2019).

[33]. G. Austern, I. G. Capeluto, Y. J. Grobman, Rationalization Methods in Computer Aided Fabrication: A Critical Review, Journal of Automation in Construction, 90 (2018) 281-293.

[34]. V. Hassani, Z. Khabazi, Form-Finding of the Metal 3D-Printed Node with Complex Geometry, LAMBERT Academic Publishing, Germany. ISBN 978-620-0-23681-4, (2019).

[35]. M.Leary, L.Merli, F.Torti, M.Mazur, M.Brandt, Optimal Topology for Additive Manufacturing: A Method for Enabling Additive Manufacture of Support-Free Optimal Structures, Journal of Materials and Design, 63 (2014) 678-690.

[36]. A. Panesar, M. Abdi, D. Hickman, I. Ashcroft, Strategies for Functionally Graded Lattice Structures Derived Using Topology Optimization for Additive Manufacturing, Journal of Additive Manufacturing, 19 (2018) 81-94.

Vahid Hassani, et. al. "A Comparison between Parametric Structural Optimization Methods and Software-Based Topology Optimization of A Rectangular Sample Under Tensile Load for Additive Manufacturing Processes."*International Journal of Engineering Research and Applications (IJERA)*, vol.11 (2), 2021, pp 37-58.